Measuring complex phenotypes: A flexible high-throughput design for micro-respirometry

Amanda N. DeLiberto[1*], Melissa K. Drown[1], Marjorie F. Oleksiak[1], Douglas L. Crawford[1]

[1] Department of Marine Biology and Ecology, Rosenstiel School of Marine and Atmospheric Science, University of Miami, Miami, FL, USA

*Corresponding author:

E-mail: amanda.deliberto@rsmas.miami.edu (AD)

Short Title: Inexpensive high-throughput micro-respirometry

Keywords

adaptation; cardiac metabolism; fatty acid; *Fundulus*; glucose; phenotype; tissue-specific metabolism; teleost

Abstract

Variation in tissue-specific metabolism between species and among individuals is thought to be adaptively important; however, understanding this evolutionary relationship requires reliably measuring this trait in many individuals. In most higher organisms, tissue specificity is important because different organs (heart, brain, liver, muscle) have unique ecologically adaptive roles. Current technology and methodology for measuring tissue-specific metabolism is costly and limited by throughput capacity and efficiency. Presented here is the design for a flexible and cost-effective high-throughput micro-respirometer (HTMR) optimized to measure small biological samples. To verify precision and accuracy, substrate specific metabolism was measured in heart ventricles isolated from a small teleost, *Fundulus heteroclitus,* and in yeast (*Saccharomyces cerevisiae*)*.* Within the system, results were reproducible between chambers and over time with both teleost hearts and yeast. Additionally, metabolic rates and allometric scaling relationships in *Fundulus* agree with previously published data measured with lower-throughput equipment. This design reduces cost, but still provides an accurate measure of metabolism in small biological samples. This will allow for high-throughput measurement of tissue metabolism that can enhance understanding of the adaptive importance of complex metabolic traits.

2

Introduction

34

35   Understanding evolution and ecological adaptation can be enhanced by combining

36   genomics with quantitative analyses of complex phenotypic traits [1]. This integrative approach

37   requires sufficient sample size (i.e. 100s to 1000s) with precise measure of phenotypes, however

38   it can be challenging to obtain economical equipment for such high-throughput quantification.

39   To address this challenge, we present an inexpensive custom design to measure metabolism in

40   small biological samples such as cell suspensions, individual tissues or possibly small organisms.

41   Metabolism is a complex trait intricated in most physiological processes and is important to

42   organismal success. Thus, metabolism is ecologically and evolutionarily important [2–11]. The

43   effect of the environment on metabolism as well as tissue-specific variation can vary

44   considerably among individuals and populations [12–18]. These and other data suggest that

45   measuring metabolism can provide insights into the ecology and evolution of organisms [5].

46   Metabolism is typically quantified via oxygen consumption rates (MO_2). Numerous

47   systems to measure MO_2 are available from companies including Unisense, PreSens, and Loligo,

48   but each has limitations with respect to technical design, throughput capacity, and cost. For small

49   biological samples, systems often have limited capacity (e.g. Oxygraph 2-K, OROBOS

50   INSTRUMENTS, Innsbruck, Austria) or require expensive reagents and disposables (e.g.,

51   Seahorse XF Analyzers, Agilent, Santa Clara, CA). Therefore, these systems are not ideal for

52   high-throughput experimental designs as it becomes time consuming and expensive to measure

53   many samples. There is a need in the field for a simple design that can measure multiple sample

54   simultaneously at a reduced cost. Here we present a design for a high-throughput micro-

55   respirometer (HTMR) that increases throughput of tissue-specific metabolism while minimizing

56   costs maintaining and maintaining efficacy. We validate the precision and accuracy of this

57   system by measuring both *Saccharomyces cerevisiae* and substrate specific metabolism in

58   *Fundulus heteroclitus* heart ventricles.

Materials and methods

Instrumentation

61   The HTMR consists of a custom external plexiglass water bath designed to enclose 1-ml

62   micro-respiration chambers (Unisense) (Fig 1A). The water bath is connected to a temperature-

63   controlled, re-circulating system, and placed on a multi-place stir plate. Each chamber contains a

64   stir bar and nylon mesh screen for mixing media while keeping tissues suspended (Fig 1B).

65   Exact chamber volumes were determined by measuring the mass (to 0.001 g) of water that

66   completely filled individual chambers with the mesh screen and stir bar. A fluorometric oxygen

67   sensor spot (PreSens) is adhered to the internal side of the chamber lid with a polymer optical

68   fiber cable affixed to each chamber lid for contactless oxygen measurement through the sensor

69   spot. All cables are connected to a 10-channel microfiber-optic oxygen meter (PreSens), which

70   uses PreSens Measurement Studio 2 software to collect oxygen data at a sampling rate of 20

71   measurements per minute. Sensors were calibrated at 0% (using 0.05 g sodium dithionite per 1

72   ml of media) and 100% air saturation (fully oxygenated media). Validation of the HTMR was

73   carried out using a four-chamber system; however, it can easily be extended to a 10-chamber

74   system as in Fig 1A.

75   **Fig 1. Ten chamber high-throughput micro-respirometer (HTMR).** (A) PreSens 10-channel oxygen meter with

76   fiber optic cables connected via contactless oxygen sensor spots in each chamber. Glass chambers are sealed in a

77   water bath for constant temperature control, positioned on a stir-plate to circulate the media within each individual

78   chamber. A temperature probe is connected and placed in the water bath to monitor temperature. (B) Individual

79   chamber design, with Unisense 1 ml micro-respiration chamber, modified with a contactless sensor spot adhered to

4

80   the inner surface of the lid and a stir bar below a nylon mesh screen. The fiberoptic cable is attached to the lid

81   adjacent to the sensor spot. (C) General schematic of experimental metabolic measurements in teleost ventricles.

82   Each ventricle is measured in each substrate for six minutes and then placed in the following substrate while

83   exchanging chamber media. Substrate conditions are measured as follows: 1) 5 mM glucose; 2) 1 mM palmitic acid;

84   3) 5 mM lactate, 5 mM hydroxybutyrate, 5 mM acetoacetate, and 0.1% ethanol; and 4) endogenous metabolism with

85   no substrate. Glycolytic enzyme inhibitors (10 mM iodoacetate and 20 mM 2-deoxyglucose) are added to fatty acid,

86   LKA, and endogenous conditions to inhibit residual glycolytic metabolism.

Metabolic rate determinations

88   The precision and accuracy of the HTMR was validated by measuring MO_2 in both yeast

89   (*Saccharomyces cerevisiae)* and teleost *(F. heteroclitus)* heart ventricles. MO_2 is measured in the

90   sealed chambers by measuring oxygen concentration at a rate of 20 measurements per minute,

91   over a six-minute period. During each daily measurement, a minimum of three blank

92   measurements, during which only media was in the chamber, were run to determine any

93   background flux. For each six-minute measurement, the last three minutes (60 datapoints) were

94   used for calculating metabolic rate. To do so, oxygen concentration was regressed against time to

95   determine the raw oxygen consumption rate ($pmol*\mu l^{-1}*min^{-1}$). Slopes were also calculated for

96   each blank measurement and averaged by chamber to quantify background flux, then subtracted

97   from each slope. Metabolic rate was measured as $MO_2 = (M_{sample} - M_{blank}) * V_{chamber} * 1/60$,

98   where MO_2 is the final metabolic rate in $pmol*s^{-1}$, M is the slope of oxygen consumption per

99   sample in $pmol*\mu l^{-1}*min^{-1}$, and V is the volume of each chamber in μl.

100   PreSens datafiles provide data per sensor with oxygen concentration ($\mu mol*L^{-1}$) at each

101   time point (minutes). An R markdown file detailing this analysis of the raw PreSens data files

102   can be found at https://github.com/ADeLiberto/FundulusGenomics.git.

5

Experimental Organisms

Fundulus heteroclitus were collected using wire minnow traps from Cape Cod, MA, Mt. Desert Island, ME, and Deer Isle, ME. Individuals were trapped on public land, and no permit was needed to catch these marine minnows for non-commercial purposes. All fish were common gardened at 20°C and salinity of 15 ppt in re-circulating aquaria for at least five months and then acclimated to 12°C or 28°C for at least two months prior to metabolic measurements. Fish were randomly selected, weighed, and then sacrificed by cervical dislocation. Heart ventricles were isolated and immediately placed in Ringer's media (1.5mM $CaCl_2$, 10 mM Tris-HCl pH 7.5, 150 mM NaCl, 5mM KCl, 1.5mM $MgSO_4$) supplemented with 5 mM glucose and 10 U/ml heparin to expel blood. Media was incubated at the measurement temperature prior to use. Ventricles were then splayed following precedent of previous cardiac metabolism measurements in *F. heteroclitus* [19]. Splaying the hearts decreases variation and increases overall oxygen consumption rates, as greater internal surface area is exposed to the substrate media [20]. After splaying, hearts were not further stimulated, as mechanical disruption or homogenization can increase variability in oxygen consumption rates [15]. All animal husbandry and experimental procedures were approved through the University of Miami Institutional Animal Care and Use Committee (Protocol # 19-045).

Methodological validation

In order to validate the HTMR performance, several parameters were tested: 1) net flux at multiple oxygen concentrations, 2) between-chamber variability in MO_2, and 3) consistency of MO_2 over time. To quantify net flux and confirm equal rates between chambers, flux was measured at multiple oxygen concentrations in each chamber. Here we define net flux as both

6

125   background oxygen consumption and oxygen diffusion into the system. Flux at 100% air

126   saturation was measured with fully oxygenated Ringer's media. To measure net flux at lower

127   oxygen saturations, Ringer's media was deoxygenated to the desired level with nitrogen gas.

128   85% air saturation was chosen because cardiac MO_2 measurements over the six minutes typically

129   deplete oxygen to approximately 92% of air saturation but do not exceed 85%. To determine net

130   flux, oxygen concentration was measured in each chamber for 10 minutes and repeated in

131   triplicate.

132   Biological repeatability between chambers was tested with yeast at 28°C. A cell

133   suspension was prepared using 1 g of yeast per 10 ml of Ringer's media supplemented with 5

134   mM glucose. In each chamber, 100 µl of the suspension was injected to account for variation in

135   chamber volume. Oxygen consumption was measured for 10 minutes in triplicate. MO_2 was

136   calculated as above to confirm there were no differences among chambers.

137   In order to assess metabolic consistency over the time-course of the experiment as well as

138   chamber repeatability, hearts from four fish were isolated, and glucose metabolism was assayed

139   in each chamber at 28°C. Hearts were randomly assigned to one of the four chambers and cycled

140   through each of them, with media exchange between each measurement. Three blank

141   measurements were run at the conclusion of the experiment. MO_2 was calculated as above and

142   then regressed against relative time of initial oxygen measurement per cycle to determine

143   metabolic rate consistency of heart tissue over time.

Substrate Specific Metabolism

145   For teleost ventricles, substrate specific metabolism was measured under four conditions:

146   1) 5 mM glucose, 2) fatty acids (1mM Palmitic acid conjugated to fatty-acid free bovine serum

7

147   albumin), 3) LKA: (5mM lactate, 5mM hydroxybutyrate, 5 mM ethyl acetoacetate, 0.1%

148   ethanol) and 4) non-glycolytic endogenous metabolism (no substrate). With the exception of

149   glucose measurements, glycolytic enzyme inhibitors (20 mM 2-deoxyglucose and 10 mM

150   iodoacetate) were added to all substrates to inhibit residual glycolytic activity. These substrate

151   concentrations are commonly used for assaying substrate metabolism in teleost ventricles [19–

152   22]. As outlined above, MO_2 was measured over six minutes for each substrate. Measurements

153   occurred at either 12°C or 28°C, the temperature at which the fish had been acclimated. After

154   measurement, hearts were placed in a media bath of the next substrate while media was

155   exchanged in each chamber. Substrate metabolism was measured in the above order for each

156   individual heart (Fig 1C).

Fatty acid saponification

158   Palmitic acid was conjugated to fatty acid-free bovine serum albumin (BSA) in order to

159   facilitate cellular uptake by the heart ventricles. A solution of 4 mM sodium palmitate and 150

160   mM NaCl was prepared and heated to 70°C until fully dissolved. A second solution of 0.68 mM

161   fatty-acid free BSA and 150 mM NaCl was prepared, sterile filtered, and warmed to 37 °C. Once

162   dissolved, equal parts hot palmitate solution was transferred in small increments to the BSA

163   solution, while stirring. The final solution was stirred for 1 hour at 37°C and stored at -20°C until

164   use. Conjugation produces a final concentration of 2 mM palmitate: 0.34 mM BSA (6:1

165   FA:BSA), which is at a 2X concentration of the final working solution used in metabolic

166   measurements.

Statistical analysis

168   Raw data processing and statistical analyses were conducted using RStudio 1.1.463.

Results

169

170   The HTMR is a simple custom design composed of a plexiglass water bath enclosing

171   micro-respiration chambers connected to a multi-channel oxygen meter (Fig 1A). For a 10-

172   chamber system, the approximate cost per chamber is $1870, including the cost of the oxygen

173   meter and stir-plate. The full cost of the system is broken down in Table 1. The oxygen meter

174   itself represents the highest cost (~$14,000 for ten inputs). followed by 1 ml glass chambers with

175   lid containing two injection ports (~$300 each). Optical-fiber cables and sensor spots combined

176   are approximately $95 each. A multi-place stir-plate is also necessary (~$900).

177   **Table 1. Cost breakdown of HTMR system**

Description	Manufacturer	Product #	Cost
10-channel microfiber-optic oxygen meter	PreSens	300000008	$13,966
O$_2$ Sensor Spots	PreSens	200001526	$26
Fiber optical cable	PreSens	200001731	$69
Glass chamber	Unisense	MR-CH1	$88
Glass chamber lid with two microinjection ports	Unisense	MR-CH INJECT LID	$183

178

Methodological validation

179

180   Net flux was tested at multiple oxygen concentrations. In the chambers, background

181   activity was negligible (2.038 pmol*s^{-1}), when flux was measured at 100% air saturation (Fig

182   2A). In contrast, the average oxygen consumption rate of *F. heteroclitus* ventricles with glucose

183   is 39.818 pmol*s^{-1}, thus flux at 100% air saturation is approximately 5%. Similarly, at 85% air

184   saturation (Fig 2B), flux was negligible (-0.324 pmol*s^{-1}), representing less than 1% of cardiac

185   glucose MO_2. In contrast, flux was somewhat high at 50% with an average flux -14.429 pmol*s^{-}

186   ^{1}, likely due to high leak (S1 Fig). However, for all three oxygen concentrations, flux was equal

187   among chambers by one-way ANOVA testing (p=0.696, p=0.643, p=0.733 at 100%, 85% and

188   50% air saturation, respectively).

189   **Fig 2. Chamber reproducibility in flux and metabolism.** Flux was measured at 100% (A), 85% (B) in all

190   four chambers of the HTMR. Additionally, MO_2 of a standardized yeast cell suspension, was measured in each

191   chamber (C). Oxygen consumption rates were calculated in pmol*s^{-1} and are represented by the mean with

192   standard error bars (n=3 for each measurement). A one-way ANOVA was used for each measurement to test

193   that there were no differences among chambers.

194   To test biological repeatability among the chambers, yeast metabolism per chamber was

195   measured. Average MO_2 was 12.502 ± 1.907 pmol*s^{-1}, and there were no significant differences

196   in metabolism between each of the chambers (ANOVA, p = 0.538; Fig 2C). This MO_2 for yeast

197   is approximately 40-fold higher than the net flux at 85% air saturation. In addition to yeast

198   measurements, heart ventricles were measured across all four chambers over a 45-minute time

199   period to validate both repeatability among chambers and that ventricles can maintain consistent

200   metabolic activity over time. Among the four replicates, there was no significant difference in

201   metabolic rate when regressed against time (linear model, p = 0.657; Fig 3A). Additionally, there

202   were no significant differences in metabolic activity among the four chambers for each heart

203   (ANOVA, p = 0.363; Fig 3B).

204   **Fig 3. Cardiac glucose metabolism over time within the HTMR.** *F. heteroclitus* ventricles (n=4) in Ringer's

205   with glucose media were rotated through the chambers and measured at 28°C. (A) Linear regression of cardiac

206   glucose MO_2 for the four replicated time periods (p=0.657) (B) Average metabolic rate per chamber,

207   represented by the mean and standard error bars (ANOVA, p = 0.164).

Substrate specific utilization

209   Heart ventricles were measured at corresponding acclimation temperatures; thus,

210   temperature represents both the physiological effects of acclimation and the direct effect of

211   temperature on MO_2. All hearts were metabolically active under each of the four substrate

212   conditions (Fig 4). For substrate specific metabolism, data was analyzed separately for

213   individuals measured at 12°C or 28°C. There is a large inter-individual variation in substrate

214   specific metabolism, which reduces the statistical power to reject the null hypothesis of no

215   difference among substrates. To avoid this type II error, we apply paired t-tests that compare

216   substrates within each individual and use Bonferroni's test to correct for multiple tests [23].

217   Glucose, FA, and LKA metabolism were significantly greater than endogenous (p=0.001,

218   Bonferroni's corrected p=0.006); except FA at 12°C (p=0.03; Bonferroni's corrected p=0.18; Fig

219   4A). Glucose metabolism was significantly greater than FA and LKA (Bonferroni's corrected

220   p=0.006) at both 12°C and 28°C. FA metabolism was significantly greater than LKA metabolism

221   at 28°C (Bonferroni's corrected p=0.006; Fig 4B) but not at 12°C (p=0.5; Fig 4A).

222   **Fig 4: Heart ventricle substrate specific metabolism.** Substrate specific ventricle MO_2 as a percent of

223   glucose consumption, represented by the mean with standard error bars. Percent glucose metabolism is relative

224   to the mean glucose metabolism of all individuals measured at each temperature. Metabolism was measured at

225   12°C (A) and 28°C (B). A paired t-test was used to compare substrate metabolism within individuals, with

226   Bonferroni test correction. Letters indicate significance levels between each substrate. At 12°C, n = 95. At

227   28°C, n = 105.

228   The $\log_{10}$ substrate specific MO_2 from Maine and Massachusetts acclimated to 12°C and

229   28°C determined here can be compared to MO_2 measured in Oleksiak *et. al* (2005) for Maine

230   individuals acclimated to 20°C using an ANCOVA with $\log_{10}$ body mass and temperature as

231   linear covariates. There were no significant differences (p = 0.55, 0.15, and 0.85 for glucose, FA

232   and LKA respectively) and the least squares fall within 5% of one another.

Allometric scaling of metabolism

234   Both body mass and heart ventricle mass were measured of each *F. heteroclitus*

235   individual measured at each temperature. The mean body mass of individuals measured at 12°C

236   and 28°C was 9.11 ± 2.87 g and 9.32 ± 2.90 g, respectively, and was not significantly different

237   between temperatures. Additionally, average ventricle masses were 0.013 ± 0.005 and 0.010 ±

238   0.004 for 12°C and 28°C, respectively and did not significantly differ between acclimation

239   temperatures. In *F. heteroclitus* body mass and heart mass are highly correlated (linear

240   regression at 12°C R^2= 0.74, p<0.0001; for 28°C, R^2= 0.66, p < 0.001) thus, body mass was used

241   to correct for variation due to mass between individuals, as done previously [24]. Body mass

242   explained a significant amount of the variation (30-70%) in metabolism among individuals for

243   all conditions (Fig 5). Variance explained by body mass (R^2), was higher at 12°C than at 28°C

244   (Fig 5, S1Table). For glucose MO_2, allometric scaling was identical (to the 2nd significant digit)

245   to previous determinations and nearly the same as in Jayasundara *et al.* (2015). Examining the

246   effect of temperature and substrates, allometric scaling coefficients (S1 Table), were between

247   0.65 to 1.29. While body mass contributed significantly to the variation between individuals,

248   there was no effect of sex on cardiac metabolism by linear regression at each substrate-

249   temperature combination. A three-way ANOVA including substrate, body mass and sex showed

12

250   no significant differences between males and females in cardiac metabolism at 12°C or 28°C (p

251   = 0.0963 and p= 0.4143, respectively).

252   **Fig 5. Allometric scaling relationship of substrate specific metabolism.** Regression of log MO_2 versus log body

253   mass with each substrate. Top panels represent fish measured at 12°C while bottom panels represent 28°C. Hearts

254   were measured as described in Fig 1 with glucose, fatty acids, LKA and endogenous metabolism. At 12°C, n= 105

255   and at 28°C n=95. For full data on regression slopes, see S1 Table.

Discussion

Design

258   The HTMR provides a simple custom design for measuring small biological samples that

259   allows higher throughput measurements at lower costs. While cost is still not negligible, the

260   system as described here, including the oxygen meter, sensors, stir control and chambers reduced

261   cost by up to 30% compared to other manufacturers. The system costs approximately 10-fold

262   less than the Agilent Seahorse and does not suffer from expensive disposable chambers and

263   reagents. Using the 10 channel PreSens meter, combined with the custom chamber design, cost

264   per chamber was approximately $1870 which was 70% and 80% of the cost compared to

265   Unisense OPTO MicroOptode and Loligo OX11875 Witrox systems, respectively. The PreSens

266   oxygen meter was primarily chosen due to the flexibility of the 10-channel system. Similar

267   multi-channel systems such as the Strathkelvin Instrument use Clark electrodes, while PreSens

268   uses smaller, more precise optical oxygen sensors. Unlike Clark electrodes, the optical sensors

269   do not consume oxygen, are less expensive and have faster response times. Additionally, the

270   fiber optical cables, and oxygen meter can be used with other sensor designs for applications

271   such as whole animal metabolism [25]. This allows additional flexibility and is more

13

272 economical, as the instrument can be used for measuring both tissue-specific, whole animal

273 metabolism and numerous applications involved with oxygen measurement. Assuming a large

274 intended sample size, with four substrate measurements per heart, this instrumentation design

275 becomes more and more economical as you increase the number of chambers, making it useful

276 for large phenotypic analyses.

277 Certain limitations were encountered while developing the multi-chamber system that are

278 important to highlight. For the HTMR, several oxygen sensors were evaluated, but the sensor

279 spots were chosen for their ease of use and durability. They are long lasting and customizable in

280 their placement, allowing for repeated use. Other sensors, such as profiling oxygen microsensor

281 probes were tested; however, they were more fragile and cumbersome to use. Temperature

282 control is also essential for consistent and repeatable measurements. Temperature has a large

283 impact on oxygen solubility; thus, precise temperature control is necessary and was closely

284 regulated and monitored during measurements.

285 Chamber mixing was another important factor to control. Without thorough mixing from

286 the stir-bars, oxygen measurements are inconsistent and inaccurate. This is an advantage of this

287 system design over other multi-well plate style oxygen readers in which the media is unstirred

288 during measurement, but instead rely on mixing prior to measurement. Continuous stirring

289 allows for longer measurement periods. The size of the mesh that holds the tissue above the stir

290 bar was also optimized: very small mesh inhibits mixing, but too large mesh would not separate

291 the tissue from the stir bar in the bottom of the chamber. Additionally, nylon mesh was used over

292 steel mesh, as it did not as readily retain air bubbles.

293 Finally, leak was tested extensively. At 85% air saturation, background flux (O_2 use not

294 associated with biological sample) was small (< 1 pmol*s^{-1}) compared to heart ventricle and

14

295   yeast MO_2. To account for any amount of flux, blank measurements were taken throughout runs

296   and corrected for in each chamber, with no significant differences in leak among chambers.

297   Initially, the Unisense microinjection lids were chosen for flexibility; however, after completing

298   tests and measurements, the manufacturers released information that this particular model was

299   less airtight than other models. For future design construction, we recommend that researchers

300   use single-port lids with a sufficient path length to further minimize leak through diffusion.

Methodological Validation

302   The HTMR is sensitive to both substrates used to fuel heart ventricle metabolism and body

303   mass. HTMR determinations were very similar to previously published data (within 5%) [19].

304   Additionally, substrate specific patterns, with highest rates supported by glucose, agree with

305   previous measurements in *F. heteroclitus* [19]. Metabolism was unaffected by the time course

306   for measuring the four substrate conditions. Ventricles continue to contract over the duration of

307   the experiment and show no significant decline in metabolic activity (Fig 2A.). Importantly,

308   body mass accounted for a significant amount of variation in these individuals following an

309   allometric scaling pattern, and the log mass against $logMO_2$ linear regression has nearly identical

310   slopes to those determined by others [15,19]. These data suggest that the system is both precise

311   because the variation among samples did not obscure substrate or body mass effects and accurate

312   in that substrate specific metabolic rates are similar to previous measures [19] and have

313   allometric scaling coefficients very similar to published data [15].

Conclusions

315   The HTMR was designed to measure metabolism in many individuals, because of the large

316   individual variation and adaptive significance of the trait. We were specifically interested in

15

317 cardiac metabolism in *F. heteroclitus*, as this species shows large inter-individual variance in

318 cardiac metabolism and the mRNAs associated with this variance [19], and these patterns may

319 hold true for many species. To better understand the physiological and evolutionary importance

320 of this variance requires many individuals which the HTMR allows. For example, in this study,

321 metabolism was quantified in approximately 200 ventricles in only 10 days. Although here the

322 system is tested only with *F. heteroclitus,* this system could easily be extended to study other

323 types of tissue-specific metabolism in many individuals. The decreased cost and efficiency of the

324 design can have countless applications, allowing for high-throughput measurement of tissue

325 metabolism that can enhance our understanding of the adaptive importance of these traits.

Acknowledgements

References

330 1. Crawford DL, Schulte PM, Whitehead A, Oleksiak MF. Evolutionary physiology and

331 genomics in the highly adaptable killifish (Fundulus heteroclitus). Compr Physiol. 2020;In

332 Press.

333 2. Wilson AC, Carlson SS, White TJ. Biochemical Evolution. Annu Rev Biochem. 1977;46:

334 573–639. Available: www.annualreviews.org

335 3. Pierce VA, Crawford DL. Phylogenetic analysis of thermal acclimation of the glycolytic

336 enzymes in the genus Fundulus. Physiol Zool. 1997/11/15. 1997;70: 597–609.

337 doi:10.1086/515879

338   4.   Bacigalupe LD, Nespolo RF, Bustamante DM, Bozinovic F. The quantitative genetics of

339   sustained energy budget in a wild mouse. Evolution (N Y). 2004/04/08. 2004;58: 421–

340   429. doi:10.1111/j.0014-3820.2004.tb01657.x

341   5.   Brown JH, Gillooly JF, Allen AP, Savage VM, West GB. Toward a metabolic theory of

342   ecology. Ecology. 2004. doi:10.1890/03-9000

343   6.   Das J. The role of mitochondrial respiration in physiological and evolutionary adaptation.

344   BioEssays. 2006;28: 890–901. doi:10.1002/bies.20463

345   7.   Crawford DL, Oleksiak MF. The biological importance of measuring individual variation.

346   J Exp Biol. 2007/04/24. 2007;210: 1613–1621. doi:10.1242/jeb.005454

347   8.   Rønning B, Jensen H, Moe B, Bech C. Basal metabolic rate: Heritability and genetic

348   correlations with morphological traits in the zebra finch. J Evol Biol. 2007/08/24.

349   2007;20: 1815–1822. doi:10.1111/j.1420-9101.2007.01384.x

350   9.   Galtier N, Jobson RW, Nabholz B, Glémin S, Blier PU. Mitochondrial whims: Metabolic

351   rate, longevity and the rate of molecular evolution. Biology Letters. Royal Society; 2009.

352   pp. 413–416. doi:10.1098/rsbl.2008.0662

353   10. Nilsson JÅ, Åkesson M, Nilsson JF. Heritability of resting metabolic rate in a wild

354   population of blue tits. J Evol Biol. 2009/08/18. 2009;22: 1867–1874. doi:10.1111/j.1420-

355   9101.2009.01798.x

356   11. Pettersen AK, Marshall DJ, White CR. Understanding variation in metabolic rate. J Exp

357   Biol. 2018/01/13. 2018;221. doi:10.1242/jeb.166876

358   12. Itazawa Y, Oikawa S. A quantitative interpretation of the metabolism-size relationship in

359   animals. Experientia. 1986;42: 152–153. doi:10.1007/BF01952441

360   13.   Itazawa Y, Oikawa S. Metabolic rates in excised tissues of carp. Experientia. 1983;39:

361   160–161. doi:10.1007/BF01958874

362   14.   Burggren W, McMahon B, Powers D. Environmental and metabolic animal physiology.

363   Environmental and metabolic animal physiology. 1991. Available:

364   https://books.google.com/books?hl=en&lr=&id=7fQvbFlQBaQC&oi=fnd&pg=PA3&dq=

365   comparative+animal+physiology,+environmental+and+metabolic+animal+physiology&ot

366   s=r9_H809WWx&sig=LbQEnkf5RZ2r5RmbsULLLvmeOl4#v=onepage&q=comparative

367   animal physiology%2C environmenta

368   15.   Jayasundara N, Kozal JS, Arnold MC, Chan SSL, Di Giulio RT. High-throughput tissue

369   bioenergetics analysis reveals identical metabolic allometric scaling for teleost hearts and

370   whole organisms. Zhang J, editor. PLoS One. 2015;10: e0137710.

371   doi:10.1371/journal.pone.0137710

372   16.   Tsuboi M, Husby A, Kotrschal A, Hayward A, Buechel SD, Zidar J, et al. Comparative

373   support for the expensive tissue hypothesis: Big brains are correlated with smaller gut and

374   greater parental investment in Lake Tanganyika cichlids. Evolution (N Y). 2015;69: 190–

375   200. doi:10.1111/evo.12556

376   17.   Sukhum K V., Freiler MK, Wang R, Carlson BA. The costs of a big brain: Extreme

377   encephalization results in higher energetic demand and reduced hypoxia tolerance in

378   weakly electric african fishes. Proc R Soc B Biol Sci. 2016;283.

379   doi:10.1098/rspb.2016.2157

380   18.   Warren DL, Iglesias TL. No evidence for the "expensive-tissue hypothesis" from an

381   intraspecific study in a highly variable species. J Evol Biol. 2012;25: 1226–1231.

18

382   doi:10.1111/j.1420-9101.2012.02503.x

383   19.   Oleksiak MF, Roach JL, Crawford DL. Natural variation in cardiac metabolism and gene

384   expression in Fundulus heteroclitus. Nat Genet. 2004/11/30. 2005;37: 67–72.

385   doi:10.1038/ng1483

386   20.   Podrabsky JE, Javillonar C, Hand SC, Crawford DL. Intraspecific variation in aerobic

387   metabolism and glycolytic enzyme expression in heart ventricles. Am J Physiol Regul

388   Integr Comp Physiol. 2000/11/18. 2000;279: R2344-8.

389   doi:10.1152/ajpregu.2000.279.6.R2344

390   21.   Sidell BD, Crockett EL, Driedzic WR. Antarctic fish tissues preferentially catabolize

391   monoenoic fatty acids. J Exp Zool. 1995;271: 73–81. doi:10.1002/jez.1402710202

392   22.   Sidell BD, Stowe DB, Hansen CA. Carbohydrate Is the Preferred Metabolic Fuel of the

393   Hagfish (Myxine glutinosa) Heart. Physiol Zool. 1984;57: 266–273.

394   doi:10.1086/physzool.57.2.30163712

395   23.   Sokal RR, Rohlf FJ. Biometry. 4th ed. W. H. Freeman and Co.; 1969.

396   24.   Pierce VA, Crawford DL. Variation in the glycolytic pathway: The role of evolutionary

397   and physiological processes. Physiol Zool. 1996;69: 489–508.

398   doi:10.1086/physzool.69.3.30164212

399   25.   Drown MK, DeLiberto AN, Crawford DL, Oleksiak MF. An Innovative Setup for High-

400   Throughput Respirometry of Small Aquatic Animals. bioRxiv. 2020; 2020.01.20.912469.

401   doi:10.1101/2020.01.20.912469

402

403

19

Supporting information

S1 Fig. Chamber reproducibility in flux at 50% air saturation.

Flux was measured at 50% air saturation in all four chambers of the HTMR. Oxygen

consumption rates were calculated in $pmol*s^{-1}$ and are represented by the mean with standard

error bars (n=3 for each measurement). A one-way ANOVA was used to test variance between

chambers (p=0.733).

S2 Fig. Chamber Leak over Time.

 Leak was tested at both high (A) and low (B) oxygen concentrations. Note the y-axes are

different values but are incrementally scaled the same.

413   **S1 Table.** Descriptive statistics of body mass regression analysis. Slope and y-intercept data of

414   the allometric relationship of body mass with substrate specific metabolism derived from a linear

415   model of the log of metabolic rate against the log of body mass per substrate by temperature.

	12°C				28°C			
	Glucose	**FA**	**LKA**	**Endogenous**	**Glucose**	**FA**	**LKA**	**Endogenous**
Slope (b)	0.7951	0.8698	0.7042	0.9339	0.6462	0.6702	1.2967	1.276
y-intercept (a)	0.7666	0.5374	0.7076	0.4484	0.9734	0.7955	-0.0004	-0.1046
R^2	0.6882	0.4726	0.5478	0.7184	0.4876	0.4464	0.2995	0.4259
N	94	80	91	90	101	99	101	89
p-value								
Slope (b)	5.19E-25	1.89E-12	5.17E-17	6.04E-26	4.78E-16	4.21E-14	1.42E-13	2.86E-08
y-intercept (a)	1.65E-25	7.13E-07	2.19E-18	3.00E-11	6.48E-28	6.69E-19	0.998	0.609
Standard Error								
Slope (b)	0.0558	0.1041	0.0678	0.0623	0.0666	0.0758	0.1513	0.2092
y-intercept (a)	0.0528	0.0996	0.064	0.059	0.0634	0.0719	0.1452	0.2038
95% Confidence Interval								
Slope (b)	0.6835 to 0.9067	0.6617 to 1.0779	0.5686 to 0.8399	0.8092 to 1.0585	0.5130 to 0.7793	0.5187 to 0.8218	0.9941 to 1.5993	0.8575 to 1.6944
y-intercept (a)	0.6610 to 0.8723	0.3382 to 0.7366	0.5796 to 0.8356	0.3304 to 0.5664	0.8465 to 1.1003	0.6518 to 0.9392	-0.2908 to 0.2901	-0.5123 to 0.3030
Significance Between Slopes*	Endogenous	NS	Endogenous	Glucose LKA	LKA Endogenous	LKA Endogenous	Glucose FA	Glucose FA

416   * Comparisons are within a single temperature between substrates based upon 95% confidence intervals presented
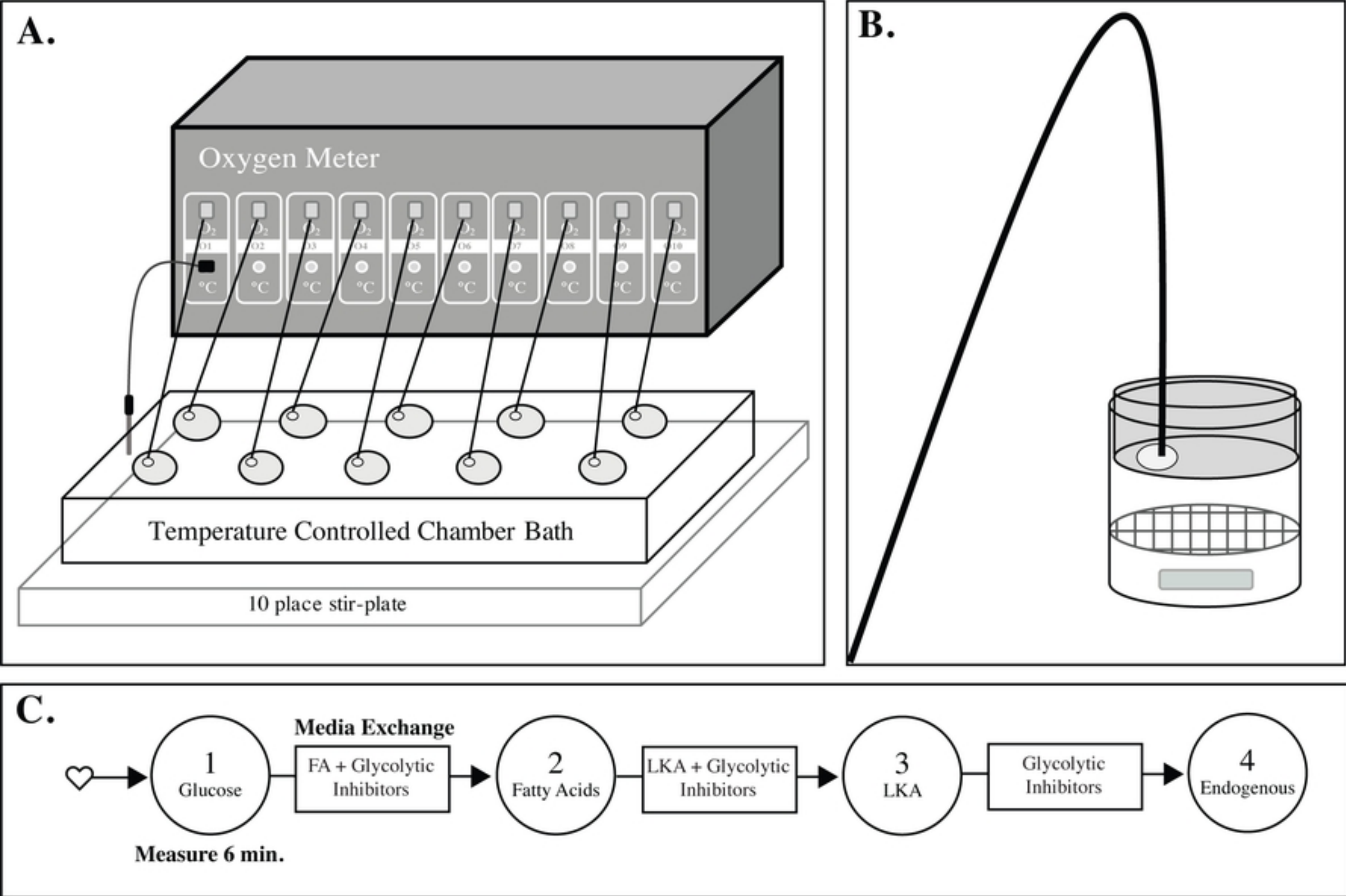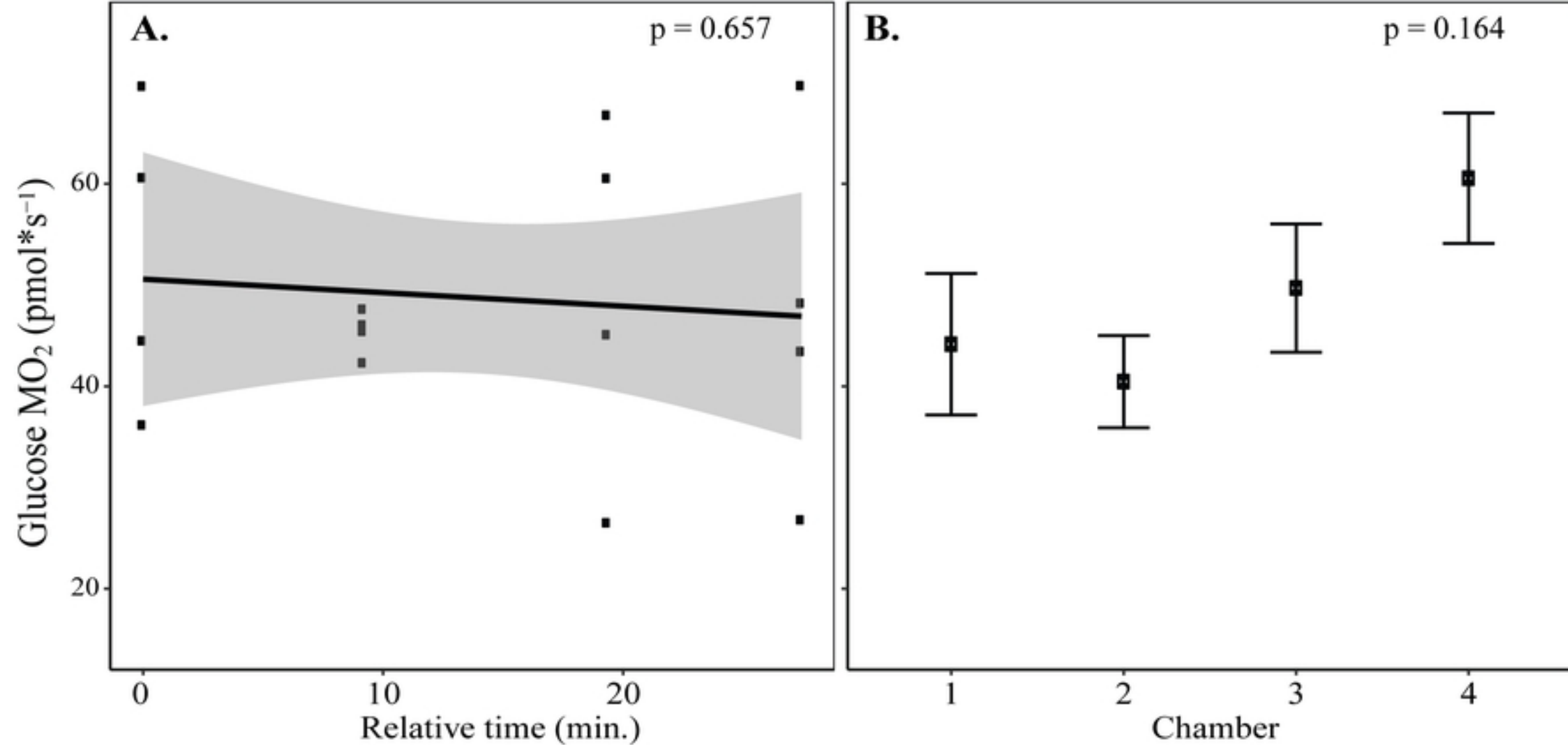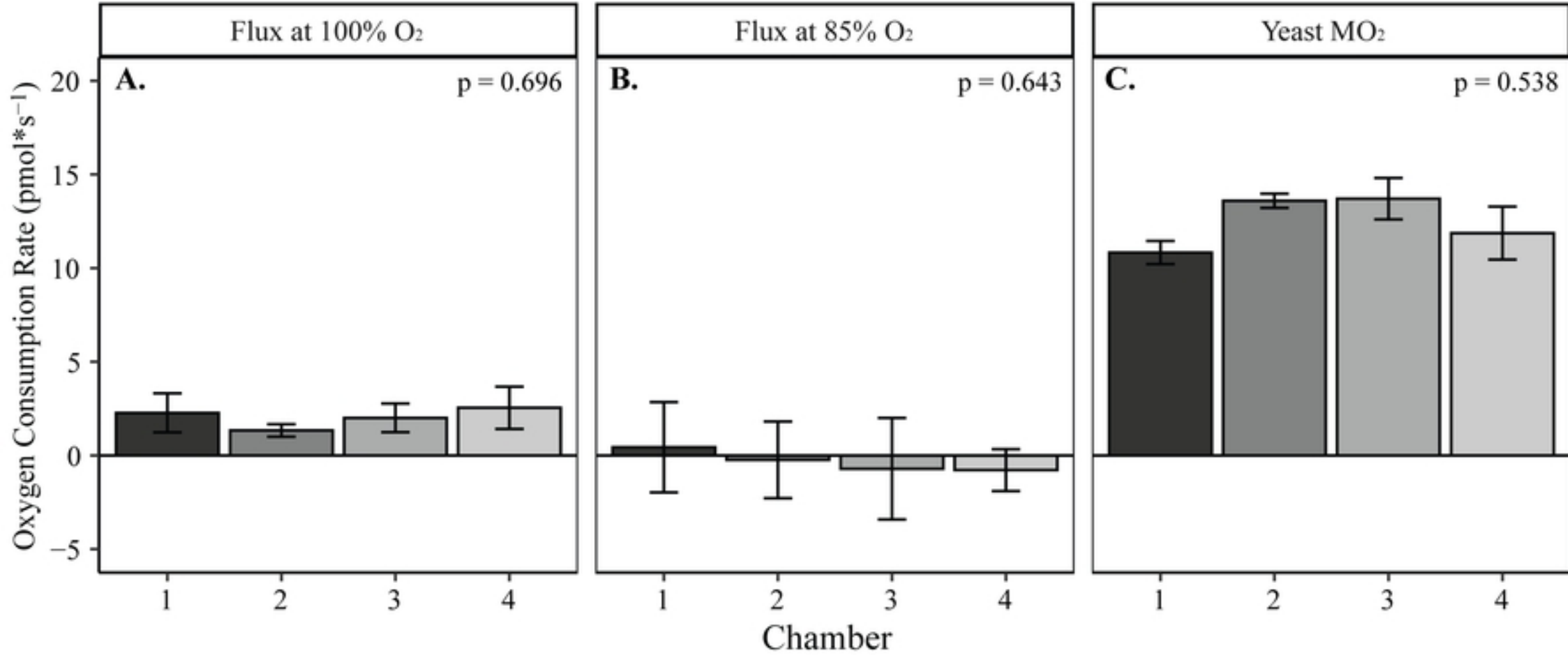
417   above.

A.

Oxygen Meter

O₁ O₂ O₃ O₄ O₅ O₆ O₇ O₈ O₉ O₁₀

Temperature Controlled Chamber Bath

10 place stir-plate

B.

C.

Media Exchange

1 Glucose → FA + Glycolytic Inhibitors → 2 Fatty Acids → LKA + Glycolytic Inhibitors → 3 LKA → Glycolytic Inhibitors → 4 Endogenous

Measure 6 min.

Fig1

Fig3

Fig2

Fig4

Fig5

S1Fig

S2Fig